
Pruning Neural Networks with Interpolative Decompositions

Jerry Chee*

Department of Computer Science
Cornell University
Ithaca, NY 14853
jc3464@cornell.edu

Megan Renz*

Department of Physics
Cornell University
Ithaca, NY 14853
mr2268@cornell.edu

Anil Damle

Department of Computer Science
Cornell University
Ithaca, NY 14853
damle@cornell.edu

Chris De Sa

Department of Computer Science
Cornell University
Ithaca, NY 14853
cdesa@cs.cornell.edu

Abstract

We introduce a principled approach to neural network pruning that casts the problem as a structured low-rank matrix approximation. Our method uses a novel application of a matrix factorization technique called the interpolative decomposition to approximate the activation output of a network layer. This technique selects neurons or channels in the layer and propagates a corrective interpolation matrix to the next layer, resulting in a dense, pruned network with minimal degradation before fine tuning. We demonstrate how to prune a neural network by first building a set of primitives to prune a single fully connected or convolution layer and then composing these primitives to prune deep multi-layer networks. Theoretical guarantees are provided for pruning a single hidden layer fully connected network. Pruning with interpolative decompositions achieves strong empirical results compared to the state-of-the-art on multiple applications from one and two hidden layer networks on Fashion MNIST to VGG and ResNets on CIFAR-10. Notably, we achieve an accuracy of $93.62 \pm 0.36\%$ using VGG-16 on CIFAR-10, with a 51% FLOPS reduction. This gains 0.02% from the full-sized model.

1 Introduction

Modern vastly over-parameterized deep networks have been shown to be effective models for a wide range of machine learning tasks. However, the same over-parameterization that seemingly helps drive their efficacy makes them computationally expensive to train and evaluate at inference time. There has recently been a significant theoretical and empirical effort to understand the necessity of over-parameterization and develop algorithmic techniques that can effectively compress (or prune) networks while retaining their performance. This work is largely driven by results that show over-parameterization may aid in training via stochastic algorithms, but that the solutions found are often highly redundant [11, 12, 30, 39] and therefore can be compressed. We develop a novel pruning methodology that uses unlabeled data to automatically exploit redundancy in trained models and perform structured pruning (i.e., removing redundant neurons/channels) that simultaneously updates the remaining network parameters. By construction, our method provides theoretical guarantees even without any additional training, though performance can typically be further improved by fine tuning.

*Equal Contribution

The core technical development in our pruning methodology is the novel use of a so-called interpolative decomposition (discussed in Section 2) to produce low-rank approximations of layers that directly incorporate the action of the activation function. By incorporating the activation function, our method differs substantially from low-rank approximation methods that directly approximate the weight matrices. Incorporation of the activation function renders the singular value decomposition (SVD) unsuitable for our task. Concisely, we are able to “propagate” low-rank factorizations through activation functions by forcing the approximation to be built using columns of the appropriate matrices directly—a process that allows for explicit sub-selection of neurons/channels. We outline the details of our technique in Section 3 for simple fully connected neural networks. Extensions to different layer types and more complex architectures can be found in Section 4.

Relative to existing techniques, our use of the interpolative decomposition provides several key advantages. In addition to sub-selecting neurons the factorization naturally provides interpolation matrices that allow us to update the weights of layers adjacent to the one currently being pruned. This allows us to directly produce a compressed network that well approximates (to any desired accuracy) the original network without any additional training—a feature we show theoretically in Section 3. We can also prune to a fixed compression level and accept the resulting degradation in accuracy. While this process requires additional data, it can be unlabeled data as our process does not require “ground truth” labels; in fact, it effectively uses pseudo-labels generated by the trained model. Another key feature of our method is that it retains the network structure—just reducing the width—and, therefore, is able to leverage the computational benefits of specific network architectures.

To complement our algorithmic developments and theoretical contributions, in Section 5 we demonstrate how our method scales to larger and more complex networks of practical interest. Importantly, we show that we can effectively prune large networks for Fashion-MNIST [58] and CIFAR-10 [32] using our scheme. Relative to competing methods we show better accuracy before fine tuning, and our methods are competitive with other state-of-the-art pruning methods after additional training is performed. Notably, our results are produced using relatively few points for the pruning process (1000 additional unlabeled data points for CIFAR-10). Our methodology suggests several key avenues for future research: we discuss those, along with limitations of our method in Section 6. To summarize, our contributions in this paper are as follows.

- **A principled pruning methodology.** We use interpolative decomposition to develop a principled approach to structured pruning of neural networks that requires only unlabeled data and allows us to directly incorporate the action of non-linear activation functions. Our methodology is applicable to a variety of layer structures and network architectures.
- **Theoretical guarantees.** We provide theoretical guarantees for the output of our pruning methodology even in the absence of additional training. This takes the form of a generalization guarantee for the pruned network (with respect to the generalization properties of the model we are pruning).
- **Practical efficacy.** We demonstrate the efficacy of our pruning methodology for networks of varying complexity. Specifically, we use Fashion MNIST and synthetic data to clearly illustrate the effectiveness of our method relative to magnitude pruning. We then provide comparisons against structured pruning methods on CIFAR-10 and show that our method performs better before fine-tuning and provides comparable results after additional training.

1.1 Related Work

Recently, there has been substantial research interest in methods for pruning neural networks, though classical magnitude pruning is still considered an effective approach [3, 11, 13, 14, 38]. One line of work concerns structured pruning of deep convolutional networks. Li et al. [33] is one of the earliest of these works which prunes channels based on their L_1 -norm. However, pruning with just the magnitudes of a trained network does not account for the possibility of duplicate neurons or channels with high magnitude. Other works have aimed to resolve these issues: one popular approach is to train with a sparsity inducing regularizer such as the L_1 or L_0 norm, and then prune small magnitude groups [27, 28, 37, 60]. Other methods aim to estimate the importance of channels. Luo, Wu, and Lin [39] greedily removes channels with the smallest effect on the next layer’s activation output. He, Zhang, and Sun [21] cast channel selection as a LASSO regression problem to determine a feature map with minimal reconstruction error of the next layer. Zhuang et al. [61] introduce a loss which encourages discrimination in the intermediate layers, and prune based on this loss. He et al. [20] calculate the geometric median of channels in a layer to select the most distinct ones. Peng et al. [50]

analyze the joint impact of pruned and kept channels on the final loss, and prune as an optimization problem. Other proposed pruning methods use reinforcement learning [22] or meta-learning [36].

Pruning with coresets [48] is the closest in spirit to our own work. The coreset algorithm provides a way to select a subset of neurons in the current layer which can approximate those in the next layer, as well as new weight connections. Mussay et al. [48] provide a sample complexity result, as well as demonstrate their method on fully connected (but not convolution) layers. Another line of work close to ours is called the filter decomposition [10, 31, 49, 55, 57, 59]: here, convolution weights are approximated with a low-rank matrix decomposition such as the SVD [10] or CP-decomposition [55].

2 Interpolative decompositions

Our pruning strategy relies on a structured low-rank approximation known as an interpolative decomposition (ID). Classically, the Singular Value Decomposition (SVD) (see, e.g., [15]) provides an optimal low-rank approximation. However, because we consider matrices that include the non-linear activation function the SVD cannot be directly used to either subselect neurons or generate new ones (since it is unclear how to propagate singular vectors backwards through the non-linearity). In contrast, an ID constructs a structured low-rank approximation of a matrix A where the basis used for the approximation is constrained to be a subset of the columns of A . For a matrix $A \in \mathbb{R}^{n \times m}$ we let $A_{\mathcal{J}, \mathcal{I}}$ denote a sub-selection of the matrix A using sets $\mathcal{J} \subset [n]$ to denote the selected rows and $\mathcal{I} \subset [m]$ to denote the selected columns; $:$ denotes a selection of all rows or columns.²

Definition 2.1 (Interpolative Decomposition). Let $A \in \mathbb{R}^{n \times m}$ and $\epsilon \geq 0$. An ϵ -accurate *interpolative decomposition* $A \approx A_{:, \mathcal{I}} T$ is a subset of columns of A , denoted with the index subset $\mathcal{I} \subset [m]$, and an associated interpolation matrix T such that

$$\|A - A_{:, \mathcal{I}} T\|_2 \leq \epsilon \|A\|_2.$$

Remarks. When computing an ID, we would like to find the smallest possible $k = |\mathcal{I}|$ such that the accuracy requirement is satisfied.³ Moreover, we would like T to have entries of reasonable magnitude and approximation error not much larger than the best possible for a given k (i.e., $\|A - A_{:, \mathcal{I}} T\|_2 = t \sigma_{k+1}(A)$ for some small $t \geq 1$). While necessarily sub-optimal, the advantage of such a factorization is that we explicitly use a subset of the columns of A to build the approximation.

IDs are well studied [8, 43], widely used in the domain of rank-structured matrices [23, 24, 25, 42, 44, 45], and are closely related to CUR decompositions [40, 56] and subset selection problems [4, 9, 54]. While these decompositions always exist, finding them optimally is a difficult task and in this work we appeal to so-called (strong) rank-revealing QR factorizations [5, 6, 7, 17, 26].

Definition 2.2 (Rank-revealing QR factorization). Let $A \in \mathbb{R}^{n \times m}$, $\ell = \min(n, m)$, and take any $k \leq \ell$. A *rank-revealing QR factorization* of A computes a permutation matrix $\Pi \in \mathbb{R}^{m \times m}$, an upper-trapezoidal matrix $R \in \mathbb{R}^{\ell \times m}$ (i.e. $R_{i,j} = 0$ if $i > j$), and a matrix $Q \in \mathbb{R}^{n \times \ell}$ with orthonormal columns (i.e., $Q^\top Q = I$) such that $A \Pi = QR$ and Q and R satisfy certain properties. Splitting Π , Q , and R into $\Pi_1 \in \mathbb{R}^{m \times k}$, $\Pi_2 \in \mathbb{R}^{m \times (m-k)}$, $Q_1 \in \mathbb{R}^{n \times k}$, $Q_2 \in \mathbb{R}^{n \times (\ell-k)}$, $R_{11} \in \mathbb{R}^{k \times k}$, $R_{12} \in \mathbb{R}^{k \times (m-k)}$, and $R_{22} \in \mathbb{R}^{(\ell-k) \times (m-k)}$ we can write

$$A [\Pi_1 \quad \Pi_2] = [Q_1 \quad Q_2] \begin{bmatrix} R_{11} & R_{12} \\ & R_{22} \end{bmatrix}. \quad (1)$$

Remarks. What makes (1) a rank-revealing QR factorization is that the permutation Π is computed to ensure that R_{11} is as well-conditioned as possible and R_{22} is as small as possible. While more formal statements of these conditions exist, we omit them here as they do not factor into our work.

Critically, for any rank-revealing QR factorization as in (1) we get a natural rank- k approximation of A with error

$$\|A - Q_1 [R_{11} \quad R_{22}] \Pi^\top\|_2 = \|R_{22}\|_2.$$

While finding the optimal rank-revealing QR factorization (i.e., minimizing the error for a given k) is closely related to a provably hard problem [9], we find the original algorithm of Businger and Golub [5] works well in practice. This routine is available in LAPACK [1, 51], can be easily incorporated into existing code, and has computational complexity $\mathcal{O}(nmk)$ when run for k steps.

²Generally, we use standard linear algebra notation and provide a detailed description in the supplement.

³We use the spectral norm in the definition, but it is natural to define an ID with respect to any matrix norm; if the norm is unitarily invariant QR factorizations still provide a suitable computational tool.

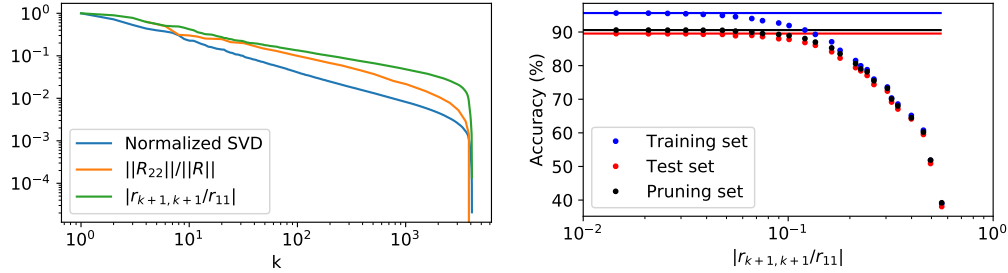


Figure 1: Left: Normalized singular value decay, $\|R_{22}\|_2/\|R\|_2$, and $|r_{k+1,k+1}/r_{1,1}|$ for a matrix from (3) from a one hidden layer network (i.e., $g(W^\top X)$) trained on Fashion MNIST. We see that the metrics generally correlate well in this setting. Right: Accuracy of a single hidden layer network pruned from width 4096 to k . The horizontal lines are the accuracy of the full sized network. The difference between pruning and test accuracy is due to a slight class imbalance in the canonical test set.

Computing interpolative decompositions Given a rank-revealing QR factorization, we can immediately construct an ID. A formal algorithmic statement is given in the supplement. We outline the method here. Let $\mathcal{I} \subset [m]$ be such that $A_{:, \mathcal{I}} = A\Pi_1$ and define an interpolation matrix

$$T = [I_k \quad R_{11}^{-1}R_{12}] \Pi^\top.$$

With this choice of $A_{:, \mathcal{I}} = Q_1R_{11}$ it follows that the error of the ID as defined by \mathcal{I} and T is $\|A - A_{:, \mathcal{I}}T\|_2 = \|R_{22}\|_2$. Picking k such that $\|R_{22}\|_2 \leq \epsilon\|A\|_2$ yields the desired relative error. Notably, since $\kappa(A_{:, \mathcal{I}}) = \kappa(R_{11})$ and $T = [I_k \quad R_{11}^{-1}R_{12}] \Pi^\top$ the desired criteria for an ID map back to those of a rank-revealing QR factorization—if R_{11} is well conditioned then the basis we use for approximation is as well and entries of T are not too large. If $\sigma_{\max}(R_{22})$ is not much larger than $\sigma_{k+1}(A)$ we get near optimal approximation accuracy.

Accuracy of the matrix approximation A key feature of using a column-pivoted QR factorization to compute an ID is that it allows us to dynamically determine the approximation rank k as a function of ϵ (in fact, Figure 1 shows the approximation error tracks that of the optimal approximation provided by the SVD). Formally, this can be accomplished by monitoring $\|R_{22}\|_2$ at each step of the column-pivoted QR algorithm. However, repeatedly computing $\|R_{22}\|_2$ is expensive and often unnecessary in practice. When using the column-pivoted QR algorithm by Businger and Golub [5] the magnitude of the diagonal entries of R are non-increasing and it is common to use $|r_{k+1,k+1}/r_{1,1}|$ as a proxy for $\|R_{22}\|_2/\|A\|_2$. While formal bounds indicate the approximation of $\|R_{22}\|_2/\sigma_1(A)$ by this quantity may be loose it is effective in practice (see Figure 1) and once a candidate k has been identified $\|R_{22}\|_2$ can be computed if desired to certify the result—if the accuracy is unacceptable k can be increased until it is. Methodologically, in some settings it may be preferable to fix k and simply accept whatever accuracy is achieved.

3 Pruning with interpolative decompositions

The core of our approach is a novel use of IDs to prune neural networks. Here we illustrate the scheme for a single fully connected layer and we extend the scheme to more complex layers (e.g., convolution layers) and deeper networks in Section 4. Consider a simple two layer (one hidden layer) fully connected neural network $h_{FC} : \mathbb{R}^d \rightarrow \mathbb{R}^c$ of width m defined as

$$h_{FC}(x; W, U) = U^\top g(W^\top x)$$

with hidden layer $W \in \mathbb{R}^{d \times m}$, output layer $U \in \mathbb{R}^{m \times c}$, and activation function g . We omit bias terms: they may be readily incorporated by adding a row to W and suitably augmenting the data.

To prune the model we will use an *unlabeled* pruning data set $\{x_i\}_{i=1}^n$ with $x_i \in \mathbb{R}^d$. Let $X \in \mathbb{R}^{d \times n}$ be the matrix such that $X_{:,i} = x_i$. Preserving the action of the two layer network to accuracy $\epsilon > 0$ on the data with fewer neurons is synonymous with finding an ϵ accurate approximation

$h_{FC}(x; W, U) \approx h_{FC}(x; \widehat{W}, \widehat{U})$ where \widehat{W} has fewer columns than W . We can do this by computing an ID of the activation output of the first layer.

Concretely, let $Z \in \mathbb{R}^{m \times n}$ be the first-layer output, i.e., $Z = g(W^\top X)$, and let $Z^\top \approx (Z^\top)_{:, \mathcal{I}}$ be a rank- k ID of Z^\top with $|\mathcal{I}| = k$ and interpolation matrix $T \in \mathbb{R}^{k \times m}$ that achieves accuracy ϵ as in Definition 2.1.⁴ Because the activation function g commutes with the sub-selection operator,

$$Z \approx T^\top Z_{\mathcal{I},:} \Leftrightarrow g(W^\top X) \approx T^\top (g(W^\top X))_{\mathcal{I},:} = T^\top g\left((W^\top X)_{\mathcal{I},:}\right) = T^\top g(W_{:, \mathcal{I}}^\top X).$$

Multiplying both sides by U^\top now gives an approximation of the original network by a pruned one,

$$h_{FC}(x; W, U) = U^\top g(W^\top X) \approx U^\top T^\top g(W_{:, \mathcal{I}}^\top X) = h_{FC}(x; W_{:, \mathcal{I}}, TU). \quad (2)$$

That is, the ID has pruned the network of width m into a dense sub-network of width k with $\widehat{W} \equiv W_{:, \mathcal{I}} \in \mathbb{R}^{d \times k}$ and $\widehat{U} \equiv TU \in \mathbb{R}^{k \times c}$. Importantly, it is not possible to use the SVD of Z^\top for this task since it is not clear how to map the dominant left singular vectors back through the activation function g to either a subset of the existing neurons or a small set of new neurons. This makes use of the ID essential.

A generalization bound for the pruned network A key feature of our ID based pruning method is that it can be used to dynamically select the width of the pruned network to maintain a desired accuracy when compared with the full model. This allows us to provide generalization guarantees for the pruned network in terms of generalization of the full model and the accuracy of the ID. We state the results for a single hidden fully connected layer with scalar output (i.e., $c = 1$) and squared loss. They can be extended to more complex networks (at the expense of more complicated dependence on the accuracy each layer is pruned to), more general Lipschitz continuous loss functions, and vector valued output. We defer all proofs to the supplementary material.

Assume $(x, y) \sim \mathcal{D}$ where $x \in \mathbb{R}^d$, $y \in \mathbb{R}$, and the distribution \mathcal{D} is supported on a compact domain $\Omega_x \times \Omega_y$. We let $\mathcal{R}_0 = \mathbb{E}_{(x, y) \sim \mathcal{D}}(\|u^\top g(W^\top x) - y\|^2)$ denote the true risk of the trained full model and $\mathcal{R}_p = \mathbb{E}_{(x, y) \sim \mathcal{D}}(\|\widehat{u}^\top g(\widehat{W}^\top x) - y\|^2)$ be the risk of the pruned model. (Since $c = 1$ we let $u \in \mathbb{R}^m$ denote the last layer.) We also define the empirical risk $\widehat{\mathcal{R}}_{ID}$ of approximating the full model with our pruned model as

$$\widehat{\mathcal{R}}_{ID} = \frac{1}{n} \sum_{i=1}^n \left| u^\top g(W^\top x_i) - \widehat{u}^\top g(\widehat{W}^\top x_i) \right|^2,$$

where $\{x_i\}_{i=1}^n$ are n i.i.d. samples from \mathcal{D} (note that we do not need labels for these samples). Using this notation, Theorem 3.1 controls the generalization error of the pruned model.

Theorem 3.1 (Single hidden layer FC). *Consider a model $h_{FC} = u^\top g(W^\top x)$ with m hidden neurons and a pruned model $\widehat{h}_{FC} = \widehat{u}^\top g(\widehat{W}^\top x)$ constructed using an ϵ accurate ID with n data points drawn i.i.d from \mathcal{D} . The risk of the pruned model \mathcal{R}_p on a data set $(x, y) \sim \mathcal{D}$ assuming \mathcal{D} is compactly supported on $\Omega_x \times \Omega$ is bounded by*

$$\mathcal{R}_p \leq \mathcal{R}_{ID} + \mathcal{R}_0 + 2\sqrt{\mathcal{R}_{ID}\mathcal{R}_0}, \quad (3)$$

where \mathcal{R}_{ID} is the risk associated with approximating the full model by a pruned one and with probability $1 - \delta$ satisfies

$$\mathcal{R}_{ID} \leq \epsilon^2 M + M(1 + \|T\|_2)^2 n^{-\frac{1}{2}} \left(\sqrt{2\zeta dm \log(dm) \log \frac{en}{\zeta dm \log(dm)}} + \sqrt{\frac{\log(1/\delta)}{2}} \right).$$

Here, $M = \sup_{x \in \Omega_x} \|u\|_2^2 \|g(W^\top x)\|_2^2$ and ζ is a universal constant that depends on g .

Theorem 3.1 is developed by considering the ID as a learning algorithm applied to the output of the full model using unlabeled pruning data. This allows us to control the risk of the pruned model in (3) in terms of the risk of the original model and additional risk introduced by the pruning method. Importantly, here we are able to control the additional risk in terms of the empirical risk of the ID (which we can control) and an additive term that decays as additional pruning data is used. Lemma 3.2 codifies this decomposition \mathcal{R}_{ID} .

⁴This means k is a function of ϵ , though it is also possible specify k and accept the resulting accuracy.

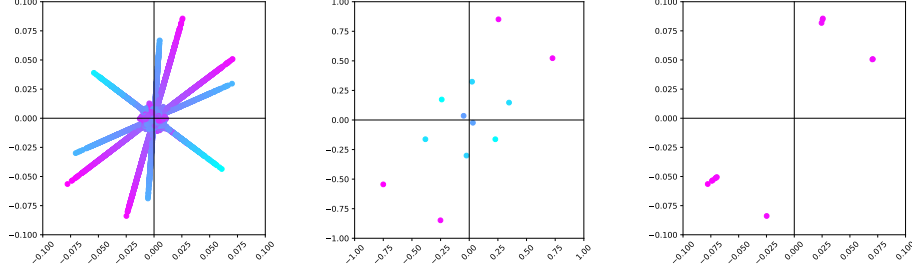


Figure 2: Neuron visualization for a simple 2-d regression task. The axes are the weights of the neurons, and the color is the bias. We have the weights trained for a full model(left) with 5000 hidden nodes. The 12 neurons kept by the ID (center) represent the function well. These are re-scaled by the magnitude of their coefficients in the second layer to display the effect of the ID. Magnitude pruning (right) keeps duplicate neurons that do not represent the function. The test loss is 0.037786 for the full model, 0.037781 for the model pruned with ID, and 0.33 magnitude-pruned model.

Lemma 3.2. *Under the assumptions of Theorem 3.1, for any $\delta \in (0, 1)$, \mathcal{R}_{ID} satisfies*

$$\mathcal{R}_{ID} \leq \widehat{\mathcal{R}}_{ID} + M(1 + \|T\|_2)^2 n^{-\frac{1}{2}} \left(\sqrt{2p \log(en/p)} + 2^{-\frac{1}{2}} \sqrt{\log(1/\delta)} \right)$$

with probability $1 - \delta$, where $M = \sup_{x \in \Omega_x} \|u\|^2 \|g(W^T x)\|^2$ and $p = \zeta dm \log(dm)$ for some universal constant ζ that depends only on the activation function.

Remarks. We believe that the second part of the bound in Lemma 3.2 is likely loose since it relies on a pseudo-dimension bound for fully connected neural networks. However, when pruning with an ID we only consider subsets of existent neurons and it is plausible that in this setting the upper bound for the pseudo-dimension could be improved.

Crucially, an immediate consequence of using an ID for pruning is that we can explicitly control \mathcal{R}_{ID} in terms of the accuracy parameter. This relation between the ID accuracy and empirical risk is given in Lemma 3.3 and is what allows us to express the risk of the pruned network in Theorem 3.1.

Lemma 3.3. *Following the notation of Theorem 3.1, an ID pruning to accuracy ϵ yields a compressed network that satisfies*

$$\widehat{\mathcal{R}}_{ID} \leq \epsilon^2 \|u\|_2^2 \|g(W^T X)\|_2^2 / n,$$

where $X \in \mathbb{R}^{d \times n}$ is a matrix whose columns are the pruning data.

This explicit control over the empirical risk of the pruned network is a key feature of ID based pruning to a fixed accuracy; though given a fixed k this could also be computed to assess the quality of an upper bound on the pruned model.

Illustrative example We created a simple synthetic data set for which we know the form of a relatively minimal model representation. Details about the data set and experiment can be found in the supplement. In Figure 2 we see that the ID well represents the original network by ignoring duplicate neurons and taking into account differences in the bias. The ID even achieves slightly better test loss than the original model. Magnitude pruning does not approximate the original model well; it keeps duplicate neurons and fails to find important information with the same number of neurons.

4 Extensions: convolutional and deep networks

Convolution layers To prune convolution layers with the ID at the channel level we reshape the output tensor into a matrix where each column represents a single output channel.⁵ After this transformation, the key idea remains the same as in Section 3. To illustrate the method, consider a simple two layer convolution neural network defined as $h_{\text{conv}}(x; W, U) = \text{conv}(U, g(\text{conv}(W, x)))$, with the convolution-layer operator conv , weight tensors W and U , and activation function g . The kernel dimension, size, stride, padding, and dilation do not change the form of the ID at the output

⁵IDs of tensors have been studied [2, 46].

Algorithm 1: ID pruning a multi-layer neural network

Input: Neural net $h(x; W^{(1)}, \dots, W^{(L)})$, layers to not prune $S \subset [L]$, pruning set X , pruning fraction α

Output: Pruned network $h(x; \widehat{W}^{(1)}, \dots, \widehat{W}^{(L)})$

```
1 set  $T^{(0)} \leftarrow I$ 
2 for  $l \in \{1 \dots L\}$  do
3    $Z \leftarrow h_{1:l}(X; W^{(1)}, \dots, W^{(l)})$  // compute activations of layer l
4   if layer  $l$  is a FC layer then
5      $(\mathcal{I}, T^{(l)}) \leftarrow \text{InterpolativeDecomposition}(Z^T; \alpha)$  if  $l \notin S$  else  $(:, I)$ 
6      $\widehat{W}^{(l)} \leftarrow T^{(l-1)} W_{:, \mathcal{I}}^{(l)}$  // sub-select neurons, multiply T of prev layer's ID
7   else if layer  $l$  is a Conv layer (or Conv+Pool) then
8      $(\mathcal{I}, T^{(l)}) \leftarrow \text{InterpolativeDecomposition}(\text{reshape}(Z); \alpha)$  if  $l \notin S$  else  $(:, I)$ 
9      $\widehat{W}^{(l)} \leftarrow \text{matmul}(T^{(l-1)}, W_{\mathcal{I}, \dots}^{(l)})$  // select channels; multiply T
10  else if layer  $l$  is a Flatten layer then
11  |  $T^{(l)} \leftarrow T^{(l-1)} \otimes I$  // expand T to have the expected size
```

channel level. Let $Z = g(\text{conv}(W, X))$ be the activation output of the first layer with unlabeled pruning data X , and define reshape as the operator which reshapes a tensor into a matrix with the output channels as columns, i.e., $\text{reshape}(Z) \in \mathbb{R}^{n_i \times m_c}$ where m_c is the number of channels and n_i is the product of all other dimensions (e.g. in the case of a 2d convolution, n_i would be width \times height \times number of examples).

We now compute⁶ a rank- k ID $\text{reshape}(Z) \approx \text{reshape}(Z)_{:, \mathcal{I}} T$. The activation function g and reshape operator both commute with the sub-selection operator, so

$$\text{reshape}(g(\text{conv}(W, X))) \approx \text{reshape}(g(\text{conv}(W, X)))_{:, \mathcal{I}} T = \text{reshape}(g(\text{conv}(W_{\mathcal{I}, \dots}, X))) T,$$

where $W_{\mathcal{I}, \dots}$ denotes an indexing sub-selection of W along its output-channel dimension. Next, we need to propagate this T into the next layer, which we can do with a “matrix multiply” by the next-layer’s weights along its input channel dimension: we call this operation matmul .⁷ With this, a little algebraic manipulation of our approximate equality above gives

$$\text{conv}(U, g(\text{conv}(W, X))) \approx \text{conv}(\text{matmul}(T, U), g(\text{conv}(W_{\mathcal{I}, \dots}, X))),$$

and so if we set $\widehat{U} = \text{matmul}(T, U)$ and $\widehat{W} = W_{\mathcal{I}, \dots}$, we can preserve the action of the two layer network with fewer channels as $h_{\text{conv}}(x; W, U) \approx h_{\text{conv}}(x; \widehat{W}, \widehat{U})$. This gives us a recipe for pruning convolution layers analogous to (2). This recipe can be directly applied to a composition of a convolution layer followed by a pooling layer [16] (or any other layer that acts independently by channel) by treating the conv layer/ pooling layer pair as a single convolution layer with a “fancy” activation function g : we just run the ID on the output post-pooling, and use that to sub-select the convolution layer’s weights. Flatten layers, for connecting to FC layers, are equally straightforward.

Deep networks The ID pruning primitives for fully connected and convolution layers can now be composed together to prune deep networks. Algorithm 1 specifies how we chain together the fully connected and convolution primitives to prune feedforward networks. A multi-layer neural network is pruned from the beginning to the end, where the ID is used to approximate the outputs of the original network. The ID pruning primitives sub-select neurons (or channels) in the current layer, and propagate the corrective interpolation matrix to the next layer. There are many ways one could prune a multi-layer network with these ID pruning primitives: we selected the approach in Algorithm 1 through empirical observations (though we do not assert that it is optimal). Discussion on the experiments which guided our design choices can be found in the supplement. Note that as a pre-processing step before running Algorithm 1, batch normalization layers [29] should be absorbed into their preceding fully-connected or convolution layers, and dropout [53] layers should be removed. We also consider residual networks [19] which consist of blocks with two or more convolution layers and a skip connection: for such residual blocks we prune all but the last layer in the block.

⁶When n_i is large we can appeal to randomized ID algorithms [43] if needed.

⁷If $T \in \mathbb{R}^{m \times n}$ and U is a weight-tensor with n input channels, then to compute $\text{matmul}(T, U)$ we: (1) reshape U to be an $n \times p$ matrix for some p , (2) multiply the reshaped matrix by T , producing a $m \times p$ matrix, and (3) reshape the result back to a tensor with m input channels and all other dimensions the same as U .

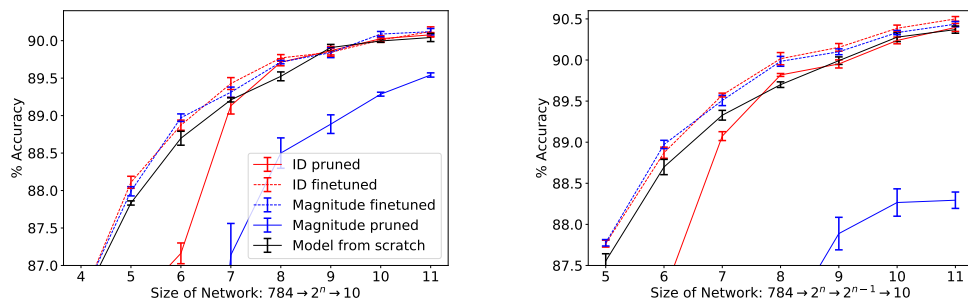


Figure 3: Accuracy for a one hidden layer (left) and two hidden layer (right) fully connected neural networks of varying size on Fashion-MNIST for ID and magnitude pruning, as well as training directly. These curves are averaged over 5 trials; error bars report uncertainty in the mean.

5 Experiments

Fashion MNIST For one and two hidden layer networks on Fashion MNIST [58] we compare the performance of ID and magnitude pruning to networks of the same size trained from scratch. Each pruning method is used to prune to half the number of neurons of the original model, and is then fine-tuned for 10 epochs. Hyper-parameter and implementation details can be found in the supplement and code. Results are shown in Figure 3; before fine-tuning the ID achieves a significantly higher test accuracy than magnitude pruning. ID pruning with fine-tuning outperforms training from scratch. At sufficiently large network sizes, ID pruning alone performs similarly to training a network from scratch. When we start to see diminishing returns from adding more neurons, the performance of the various methods begin to converge.

CIFAR-10 We analyze the performance of ID pruning against several benchmark structured pruning methods using the CIFAR-10 data set [32] with VGG [52] and ResNets [19]. The ID uses a held-out pruning set of 1000 data points; a reasonable size. Full hyper-parameter details can be found in the supplement and code. First we compare the ID against structured magnitude pruning [33] as implemented by Liu et al. [38]. Table 1 gives the results before and after fine-tuning. ID pruning better mitigates network degradation as it achieves higher test accuracy before fine-tuning. After the same amount of fine-tuning, IDs still are superior. Note FLOPs reduction = $1 - (\text{pruned} / \text{original})$.

Table 1: Results on CIFAR-10 against structured magnitude pruning [33, 38] before and after fine-tuning. We follow pruning configurations [33] which specify layer-wise pruning fractions and layers to skip. Accuracies are reported as mean and standard deviation over 5 independent trials.

Model	Approach	Baseline	Pruned		
		Acc. (%)	Acc. (%) Before FT	Acc. (%) After FT	FLOPs Reduction
VGG-16	Mag (our-impl)	93.60 (± 0.29)	64 (± 15)	93.56 (± 0.31)	34%
	ID (ours)		93.30 (± 0.16)	93.33 (± 0.19)	(Cfg.-A)
ResNet-56	Mag (our-impl)	93.04 (± 0.25)	91.68 (± 0.38)	92.84 (± 0.20)	10%
	ID (ours)		92.37 (± 0.29)	93.01 (± 0.22)	(Cfg.-A)
	Mag (our-impl)		75 (± 11)	92.63 (± 0.26)	28%
	ID (ours)		88.16 (± 1.0)	92.80 (± 0.22)	(Cfg.-B)

Next we compare the ID to other structured pruning methods, in Table 2. We prune a constant fraction of channels in each layer to achieve 50% FLOPs reduction (skipping certain layers in the ResNet as described previously). We implement FPGM [20] on our trained models. The ID achieves near state-of-the-art accuracy on VGG-16 for a FLOPs reduction of 51% and performs comparably to state-of-the-art for ResNet-56. Note that all of the compared structured pruning methods [20, 37,

60] fine-tune approximately the same amount as their original training process. We believe the large amount of fine-tuning is why we see very similar accuracies for FPGM and the ID.⁸ In addition these methods either require training with a specialized regularizer [34, 37, 60] or use other specialized training techniques [20]. As we have seen, IDs can prune a generically trained model in a principled manner with minimal accuracy degradation before fine-tuning. The complexity of fine-tuning can obfuscate the relative performance of different pruning methods. As such, comparing accuracies before fine-tuning (when possible) is a potentially clearer way to compare pruning methods. Table 3 gives the accuracies of FPGM [20] and the ID before fine-tuning. We observe that pruning with the ID is significantly better at preserving the original network, even at a greater pruning level (VGG-16).

Table 2: Results on CIFAR-10 against other structured pruning methods. Accuracies for our experiments are reported as mean and standard deviation over 5 independent trials.

Model	Approach	Baseline	Pruned		
		Acc. (%)	Acc. (%)	Acc. Drop (%)	FLOPs Reduction
VGG-16	FPGM [20] (our-impl)	93.60 (± 0.29)	93.82 (± 0.17)	-0.22	34%
	NS [37]	93.66	93.80	-0.24	51%
	Polar [60]	93.88	93.92	-0.04	54%
	Filter [34]	94.02	93.77	0.25	24%
	ID (ours)	93.60 (± 0.29)	93.62 (± 0.36)	-0.02	51%
ResNet-56	FPGM [20] (our-impl)	93.04 (± 0.25)	92.80 (± 0.11)	0.24	53%
	NS [37] ([60]-impl)	93.80	93.27	0.53	48%
	Polar [60]	93.80	93.83	-0.03	47%
	Filter [34]	92.95	93.92	-0.97	50%
	ID (ours)	93.04 (± 0.25)	92.80 (± 0.19)	0.25	50%

Table 3: Results on CIFAR-10 against FPGM [20] before fine-tuning. Accuracies are reported as mean and standard deviation over 5 independent trials.

Model	Approach	Baseline	Pruned	
		Acc. (%)	Acc. Before FT (%)	FLOPs Reduction
VGG-16	FPGM [20] (our-impl)	93.60 (± 0.29)	64 (± 10)	34%
	ID (ours)		89.76 (± 0.39)	51%
ResNet-56	FPGM [20] (our-impl)	93.04 (± 0.25)	11.1 (± 1.6)	53%
	ID (ours)		69.7 (± 2.1)	50%

6 Discussion: limitations and future work

Our method comes with several limitations and possible extensions for future work. It is not clear how to extend our method beyond feedforward networks, such as to recurrent networks. We provide theory showing the ID preserves loss, but currently do not consider other metrics such as sub-class loss. Our theory requires that the unlabeled pruning set be from the same distribution as the test set. It is also possible that we are introducing over-fitting in some way that generates less effectively trainable models. We cannot make claims about the prunability of a given model. It is possible that the k which satisfies our ϵ -accuracy condition is the full width of the network.

In future work, we will explore ways to modify the training process to create models that are more amenable to pruning, a common approach [27, 28, 37, 60]. We have observed that the type of layer and position in the network effects its prunability. However, we do not yet fully understand how to select ϵ to account for these factors. Our method shows promise at revealing the natural structure of

⁸We use the fine-tuning hyper-parameters from FPGM [20].

the network at different layers; this understanding could be used to measure the importance of the information in each layer to the learned model.

Acknowledgments and Disclosure of Funding

This research was supported in part by NSF Award DMS-1830274 and NSF Award NSF IIS-2046760, as well as by a gift from SambaNova Systems.

References

- [1] E. Anderson et al. *LAPACK Users' Guide*. Third. Philadelphia, PA: SIAM, 1999.
- [2] David J. Biagioni, Daniel Beylkin, and Gregory Beylkin. "Randomized interpolative decomposition of separated representations". In: *Journal of Computational Physics* 281 (2015), pp. 116–134.
- [3] Davis Blalock et al. "What is the state of neural network pruning?" In: *arXiv preprint arXiv:2003.03033* (2020).
- [4] Christos Boutsidis, Michael W Mahoney, and Petros Drineas. "An improved approximation algorithm for the column subset selection problem". In: *Proceedings of the twentieth annual ACM-SIAM symposium on Discrete algorithms*. SIAM. 2009, pp. 968–977.
- [5] Peter Businger and Gene H Golub. "Linear least squares solutions by Householder transformations". In: *Numerische Mathematik* 7.3 (1965), pp. 269–276.
- [6] Tony F Chan and Per Christian Hansen. "Some applications of the rank revealing QR factorization". In: *SIAM Journal on Scientific and Statistical Computing* 13.3 (1992), pp. 727–741.
- [7] Shivkumar Chandrasekaran and Ilse CF Ipsen. "On rank-revealing factorisations". In: *SIAM J. on Matrix Anal. and Apps.* 15.2 (1994), pp. 592–622.
- [8] H. Cheng et al. "On the compression of low rank matrices". In: *SIAM Journal on Scientific Computing* 26.4 (2005), pp. 1389–1404.
- [9] Ali Civril and Malik Magdon-Ismail. "On selecting a maximum volume sub-matrix of a matrix and related problems". In: *Theoretical Computer Science* 410.47-49 (2009), pp. 4801–4811.
- [10] Emily Denton et al. "Exploiting Linear Structure Within Convolutional Networks for Efficient Evaluation". In: *Advances in neural information processing systems*. 2014.
- [11] Jonathan Frankle and Michael Carbin. "The Lottery Ticket Hypothesis: Finding Sparse, Trainable Neural Networks". In: *International Conference on Learning Representations*. 2018.
- [12] Jonathan Frankle et al. "Linear mode connectivity and the lottery ticket hypothesis". In: *International Conference on Machine Learning*. PMLR. 2020, pp. 3259–3269.
- [13] Jonathan Frankle et al. "Pruning Neural Networks at Initialization: Why are We Missing the Mark?" In: *arXiv preprint arXiv:2009.08576* (2020).
- [14] Trevor Gale, Erich Elsen, and Sara Hooker. "The state of sparsity in deep neural networks". In: *arXiv preprint arXiv:1902.09574* (2019).
- [15] G. H. Golub and C. F. Van Loan. *Matrix computations*. third. Baltimore: Johns Hopkins Univ. Press, 1996.
- [16] Ian Goodfellow, Yoshua Bengio, and Aaron Courville. *Deep learning*. MIT press, 2016.
- [17] M. Gu and S. Eisenstat. "Efficient Algorithms for Computing a Strong Rank-Revealing QR Factorization". In: *SIAM J. Sci. Comput.* 17.4 (1996), pp. 848–869.
- [18] Nick Harvey, Christopher Liaw, and Abbas Mehrabian. "Nearly-tight VC-dimension bounds for piecewise linear neural networks". In: *Proceedings of the 2017 Conference on Learning Theory*. Ed. by Satyen Kale and Ohad Shamir. Vol. 65. Proceedings of Machine Learning Research. PMLR, July 2017, pp. 1064–1068. URL: <http://proceedings.mlr.press/v65/harvey17a.html>.
- [19] Kaiming He et al. "Deep Residual Learning for Image Recognition". In: *Proceedings of the 29th IEEE Conference on Computer Vision and Patter Recognition*. 2016.
- [20] Yang He et al. "Filter Pruning via Geometric Median for Deep Convolutional Neural Networks Acceleration". In: *Conference on Computer Vision and Patter Recognition*. 2019.

- [21] Yihui He, Xiangyu Zhang, and Jian Sun. “Channel Pruning for Accelerating Very Deep Neural Networks”. In: *International Conference on Computer Vision*. 2017.
- [22] Yihui He et al. “AMC: AutoML for Model Compression and Acceleration on Mobile Devices”. In: *European Conference on Computer Vision*. 2018.
- [23] K.L. Ho and L. Greengard. “A Fast Direct Solver for Structured Linear Systems by Recursive Skeletonization”. In: *SIAM Journal on Scientific Computing* 34.5 (2012), A2507–A2532. DOI: 10.1137/120866683.
- [24] K.L. Ho and L. Ying. “Hierarchical Interpolative Factorization for Elliptic Operators: Integral Equations”. In: *Communications on Pure and Applied Mathematics* (2015). ISSN: 1097-0312. DOI: 10.1002/cpa.21577. URL: <http://dx.doi.org/10.1002/cpa.21577>.
- [25] Kenneth L Ho and Lexing Ying. “Hierarchical interpolative factorization for elliptic operators: differential equations”. In: *Communications on Pure and Applied Mathematics* 69.8 (2016), pp. 1415–1451.
- [26] Yoo Pyo Hong and C-T Pan. “Rank-revealing QR factorizations and the singular value decomposition”. In: *Mathematics of Computation* 58.197 (1992), pp. 213–232.
- [27] Zehao Huang and Naiyan Wan. “Data-Driven Sparse Structure Selection for Deep Neural Networks”. In: *European Conference on Computer Vision*. 2018.
- [28] Hai Li Huanrui Yang Wei Wen. “DeepHoyer: Learning Sparser Neural Network with Differentiable Scale-Invariant Sparsity Measures”. In: *International Conference on Learning Representations*. 2020.
- [29] Sergey Ioffe and Christian Szegedy. “Batch Normalization: Accelerating Deep Network Training by Reducing Internal Covariate Shift”. In: *Proceedings of the 32nd International Conference on Machine Learning*. Ed. by Francis Bach and David Blei. Vol. 37. Proceedings of Machine Learning Research. Lille, France: PMLR, July 2015, pp. 448–456.
- [30] Max Jaderberg, Andrea Vedaldi, and Andrew Zisserman. “Speeding up Convolutional Neural Networks with Low Rank Expansions”. In: *Proceedings of the British Machine Vision Conference*. BMVA Press. 2014.
- [31] Max Jaderberg, Andrea Vedaldi, and Andrew Zisserman. “Speeding up Convolutional Neural Networks with Low Rank Expansions”. In: *British Machine Vision Conference*. 2014.
- [32] Alex Krizhevsky and Geoffrey Hinton. “Learning Multiple Layers of Features from Tiny Images”. In: *Technical Report* (2009).
- [33] Hao Li et al. “Pruning Filters for Efficient Convnets”. In: *International Conference on Learning Representations*. 2017.
- [34] Yawei Li et al. “Learning Filter Basis for Convolutional Neural Network Compression”. In: *International Conference on Computer Vision*. 2019.
- [35] Edo Liberty et al. “Randomized algorithms for the low-rank approximation of matrices”. In: *Proceedings of the National Academy of Sciences* 104.51 (2007), pp. 20167–20172.
- [36] Zechun Liu et al. “MetaPruning: Meta Learning for Automatic Neural Network Channel Pruning”. In: *International Conference on Computer Vision*. 2019.
- [37] Zhuang Liu et al. “Learning Efficient Convolutional Networks through Network Slimming”. In: *International Conference on Computer Vision*. 2017.
- [38] Zhuang Liu et al. “Rethinking the Value of Network Pruning”. In: *International Conference on Learning Representations*. 2019.
- [39] Jian-Hao Luo, Jianxin Wu, and Weiyao Lin. “Thinet: A filter level pruning method for deep neural network compression”. In: *Proceedings of the IEEE international conference on computer vision*. 2017, pp. 5058–5066.
- [40] Michael W Mahoney and Petros Drineas. “CUR matrix decompositions for improved data analysis”. In: *Proceedings of the National Academy of Sciences* 106.3 (2009), pp. 697–702.
- [41] Martín Abadi et al. *TensorFlow: Large-Scale Machine Learning on Heterogeneous Systems*. Software available from tensorflow.org. 2015. URL: <http://tensorflow.org/>.
- [42] Per-Gunnar Martinsson and V. Rokhlin. “A Fast Direct Solver for Boundary Integral Equations in Two Dimensions”. In: *J. Comput. Phys.* 205.1 (May 2005), pp. 1–23. ISSN: 0021-9991. DOI: 10.1016/j.jcp.2004.10.033. URL: <http://dx.doi.org/10.1016/j.jcp.2004.10.033>.

- [43] Per-Gunnar Martinsson, Vladimir Rokhlin, and Mark Tygert. “A randomized algorithm for the decomposition of matrices”. In: *Applied and Computational Harmonic Analysis* 30.1 (2011), pp. 47–68.
- [44] Per-Gunnar Martinsson. *Fast Direct Solvers for Elliptic PDEs*. Philadelphia, PA: Society for Industrial and Applied Mathematics, 2019. DOI: 10.1137/1.9781611976045. eprint: <https://epubs.siam.org/doi/pdf/10.1137/1.9781611976045>. URL: <https://epubs.siam.org/doi/abs/10.1137/1.9781611976045>.
- [45] Victor Minden et al. “A recursive skeletonization factorization based on strong admissibility”. In: *Multiscale Modeling & Simulation* 15.2 (2017), pp. 768–796.
- [46] Rachel Minster, Arvind K. Saibaba, and Misha E. Kilmer. “Randomized Algorithms for Low-Rank Tensor Decompositions in the Tucker Format”. In: *SIAM J. MATH. DATA SCI.* 2.1 (2020), pp. 189–215.
- [47] Mehryar Mohri, Afshin Rostamizadeh, and Ameet Talwalkar. *Foundations of Machine Learning*. 2nd ed. MIT press, 2018.
- [48] Ben Mussay et al. “Data-Independent Neural Pruning via Coresets”. In: *International Conference on Learning Representations*. 2020.
- [49] Bo Peng et al. “Extreme network compression via filter group approximation”. In: *European Conference on Computer Vision*. 2018.
- [50] Hanyu Peng et al. “Collaborative Channel Pruning for Deep Networks”. In: *International Conference on Machine Learning*. 2019.
- [51] Gregorio Quintana-Ortí, Xiaobai Sun, and Christian H. Bischof. “A BLAS-3 Version of the QR Factorization with Column Pivoting”. In: *SIAM J. on Sci. Comp.* 19.5 (1998), pp. 1486–1494. DOI: 10.1137/S1064827595296732.
- [52] Karen Simonyan and Andrew Zisserman. “Very deep convolutional networks for large-scale image recognition”. In: *International Conference on Learning Representations*. 2015.
- [53] Nitish Srivastava et al. “Dropout: a simple way to prevent neural networks from overfitting”. In: *The journal of machine learning research* 15.1 (2014), pp. 1929–1958.
- [54] Joel A Tropp. “Column subset selection, matrix factorization, and eigenvalue optimization”. In: *Proceedings of the twentieth annual ACM-SIAM symposium on Discrete algorithms*. SIAM. 2009, pp. 978–986.
- [55] VadimLebedev et al. “Speeding-up convolutional neural networks using fine-tuned cp-decomposition”. In: *International Conference on Learning Representations*. 2015.
- [56] Sergey Voronin and Per-Gunnar Martinsson. “Efficient algorithms for cur and interpolative matrix decompositions”. In: *Advances in Computational Mathematics* 43.3 (2017), pp. 495–516.
- [57] Min Wang, Baoyuan Liu, and Hassan Foroosh. “Factorized convolutional neural networks”. In: *International Conference on Computer Vision*. 2017.
- [58] Han Xiao, Kashif Rasul, and Roland Vollgraf. “Fashion-MNIST: a Novel Image Dataset for Benchmarking Machine Learning Algorithms”. In: *arXiv:1708.07747* (2017).
- [59] Xiangyu Zhang et al. “Accelerating very deep convolutional networks for classification and detection”. In: *IEEE Transactions on Pattern Analysis and Machine Intelligence*. 2015.
- [60] Tao Zhuang et al. “Neuron-level Structured Pruning using Polarization Regularizer”. In: *Advances in neural information processing systems*. 2020.
- [61] Zhuangwei Zhuang et al. “Discrimination-aware Channel Pruning for Deep Neural Networks”. In: *Advances in neural information processing systems*. 2018.

A Notation

Matrices are denoted with capital letters such as A , and vectors with lower case a . In situations where we partition a matrix into pieces, the partitions will be referred to as A_{ij} . Individual entries in a matrix will be referred to as lower case letters with two subscripts, a_{ij} . $\sigma_k(A)$ denotes the k -th leading singular value of A , and $\kappa(A)$ the condition number. For a matrix $A \in \mathbb{R}^{n \times m}$ we let $A_{\mathcal{J}, \mathcal{I}}$ denote a sub-selection of the matrix A using sets $\mathcal{J} \subset [n]$ to denote the selected rows and $\mathcal{I} \subset [m]$ to denote the selected columns; $:$ denotes a selection of all rows or columns.

B Fixed-rank interpolative decompositions

As stated in Section 2, a formal algorithmic statement is given for computing fixed-rank interpolative decompositions.

Algorithm 2: Interpolative Decomposition

Input: matrix $A \in \mathbb{R}^{n \times m}$, rank k

Output: interpolative decomposition $A_{:,1:k} T$

1 Compute column-pivoted QR factorization

$$A [\quad] = [Q_1 \quad Q_2] \begin{matrix} R_{11} & R_{12} \\ & R_{22} \end{matrix} ;$$

where $Q_1 \in \mathbb{R}^{m \times k}$, $R_{11} \in \mathbb{R}^{k \times k}$, $R_{12} \in \mathbb{R}^{k \times (m-k)}$, and remaining dimensions as required.

2 $A_{:,1:k} = A [\quad]$

3 $T = \begin{bmatrix} I_k & R_{11}^{-1} R_{12} \\ & R_{22} \end{bmatrix}$

C Proofs

Theorem 3.1. Consider a model $\mathbb{h}_{FC} = \mathbf{u}^\top g(\mathcal{W}^\top \mathbf{x})$ with m hidden neurons and a pruned model $\hat{\mathbb{h}}_{FC} = \mathbf{b}^\top g(\mathcal{W}^\top \mathbf{x})$ constructed using an accurate ID with n data points drawn i.i.d from \mathcal{D} . The risk of the pruned model R_p on a data set $(\mathbf{x}; \mathbf{y}) \in \mathcal{D}$ assuming \mathcal{D} is compactly supported on \mathcal{X} is bounded by

$$R_p \leq R_{ID} + R_0 + 2 \sqrt[p]{R_{ID} R_0};$$

where R_{ID} is the risk associated with approximating the full model by a pruned one and with probability $1 - \delta$ satisfies

$$R_{ID} \leq 2M + M(1 + kT k_2)^2 n^{-\frac{1}{2}} \sqrt{\frac{r}{2dm \log(dm) \log \frac{en}{dm \log(dm)}}} + \frac{r \log(1/\delta)}{2} ;$$

Here, $M = \sup_{\mathbf{x} \in \mathcal{X}} \|\mathbf{k}\|_2^2 \mathbf{k} g(\mathcal{W}^\top \mathbf{x}) k_2^2$ and r is a universal constant that depends on \mathcal{D}

Proof. We can write the risk for this network as

$$R_p = E(\mathbf{k} \mathbf{b}^\top g(\mathcal{W}^\top \mathbf{x}) - \mathbf{y})^2);$$

and adding and subtract the original network yields

$$\begin{aligned} E(\mathbf{k} \mathbf{b}^\top g(\mathcal{W}^\top \mathbf{x}) - \mathbf{y})^2 &= E(\mathbf{k} (\mathbf{b}^\top g(\mathcal{W}^\top \mathbf{x}) - \mathbf{u}^\top g(\mathcal{W}^\top \mathbf{x})) + (\mathbf{u}^\top g(\mathcal{W}^\top \mathbf{x}) - \mathbf{y}))^2 \\ &= E((\mathbf{k} (\mathbf{b}^\top g(\mathcal{W}^\top \mathbf{x}) - \mathbf{u}^\top g(\mathcal{W}^\top \mathbf{x})) + \mathbf{k} (\mathbf{u}^\top g(\mathcal{W}^\top \mathbf{x}) - \mathbf{y}))^2) \\ &= E(\mathbf{k} (\mathbf{b}^\top g(\mathcal{W}^\top \mathbf{x}) - \mathbf{u}^\top g(\mathcal{W}^\top \mathbf{x}))^2) \\ &\quad + E(2\mathbf{k} (\mathbf{b}^\top g(\mathcal{W}^\top \mathbf{x}) - \mathbf{u}^\top g(\mathcal{W}^\top \mathbf{x})) \mathbf{k} (\mathbf{u}^\top g(\mathcal{W}^\top \mathbf{x}) - \mathbf{y})) \\ &\quad + E(\mathbf{k} (\mathbf{u}^\top g(\mathcal{W}^\top \mathbf{x}) - \mathbf{y})^2) \\ &= R_{ID} + 2 \sqrt[p]{R_{ID} R_0} + R_0; \end{aligned}$$

Now, we bound R_{ID} by considering the interpolative decomposition to be a learning algorithm learning the function $\mathbf{u}^\top g(\mathcal{W}^\top \mathbf{X})$. Specifically, we use Lemma 3.2 to bound R_{ID} as

$$R_{ID} \leq \hat{R}_{ID} + M(1 + kT k_2)^2 n^{-\frac{1}{2}} \sqrt{\frac{p}{2p \log(en/p)} + 2 \sqrt[p]{\frac{p}{\log(1/\delta)}}} ;$$

where p is the pseudo-dimension. We can then use Lemma 3.3 to bound the empirical risk of the interpolative decomposition as

$$\hat{R}_{ID} \leq 2 \mathbf{k} \mathbf{k}_2^2 \mathbf{k} g(\mathcal{W}^\top \mathbf{X}) k_2^2 = n;$$

and it follows that

$$\widehat{\mathcal{R}}_{ID} \leq \epsilon^2 \sup_{x \in \Omega_x} \|u\|_2^2 \|g(W^T x)\|_2^2.$$

□

Lemma 3.2. *Under the assumptions of Theorem 3.1, for any $\delta \in (0, 1)$, \mathcal{R}_{ID} satisfies*

$$\mathcal{R}_{ID} \leq \widehat{\mathcal{R}}_{ID} + M(1 + \|T\|_2)^2 n^{-\frac{1}{2}} \left(\sqrt{2p \log(en/p)} + 2^{-\frac{1}{2}} \sqrt{\log(1/\delta)} \right)$$

with probability $1 - \delta$, where $M = \sup_{x \in \Omega_x} \|u\|_2^2 \|g(W^T x)\|_2^2$ and $p = \zeta dm \log(dm)$ for some universal constant ζ that depends only on the activation function.

Proof. Considering the interpolative decomposition as a learning algorithm to learn $u^\top g(W^\top X)$, we can use Theorem 11.8 in [47] to bound the risk on the data distribution. Given a maximum on the loss function η , and the ReLU activation function,

$$\mathcal{R}_{ID} \leq \widehat{\mathcal{R}}_{ID} + \frac{\eta}{n^{1/2}} (\sqrt{2p \log en/p} + 2^{-1/2} \sqrt{\log(1/\delta)})$$

with probability $(1 - \delta)$.⁹ Here, the constant η is bounded by Lemma C.1. Bartlett et al. [18] show that the p-dimension for a ReLU network is $O(\mathcal{W}L \log(\mathcal{W}))$ where \mathcal{W} is the number of weights and L is the number of layers. Here, that translates to $p = \zeta dm \log(dm)$ for some constant ζ that depends only on the choice of activation function. □

Lemma 3.3. *Following the notation of Theorem 3.1, an ID pruning to accuracy ϵ yields a compressed network that satisfies*

$$\widehat{\mathcal{R}}_{ID} \leq \epsilon^2 \|u\|_2^2 \|g(W^T X)\|_2^2 / n,$$

where $X \in \mathbb{R}^{d \times n}$ is a matrix whose columns are the pruning data.

Proof.

$$\widehat{\mathcal{R}}_{ID} = \frac{1}{n} \sum_{i=1}^n |u^\top g(W^\top x_i) - \widehat{u}^\top g(\widehat{W}^\top x_i)|^2 \quad (4)$$

Here, we can appeal to our definition of the ID to bound each term in the sum.

$$|u^\top g(W^\top x_i) - \widehat{u}^\top g(\widehat{W}^\top x_i)| = |u^\top g(W^\top x_i) - u^\top T^\top g(P^\top W^\top x_i)| \quad (5)$$

By our definition of an ϵ -accurate interpolative decomposition,

$$|u^\top g(W^\top x_i) - \widehat{u}^\top g(\widehat{W}^\top x_i)| \leq \epsilon \|u\| \|g(W^\top x_i)\| \quad (6)$$

Therefore,

$$\widehat{\mathcal{R}}_{ID} \leq \frac{1}{n} \epsilon^2 \|u\|^2 \|g(W^T X)\|^2 \quad (7)$$

□

Lemma C.1. *The maximum η of the loss function associated with approximating the full network with the pruned one is bounded as*

$$\eta \leq \sup_{x \in \Omega_x} \|u\|_2^2 \|g(W^T x)\|_2^2 (1 + \|T\|)^2$$

⁹e is the base of the natural log.

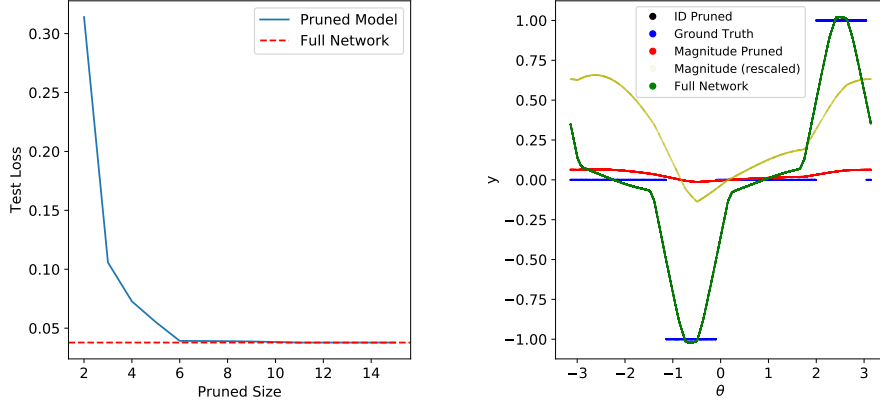


Figure 4: A plot of loss v.s. number of neurons kept (left) and a plot of the function evaluation for the full network, ID pruning, and magnitude pruned model (right). The data is drawn from the unit circle, and we parameterize X in terms of an angle θ . To see more detail in the magnitude pruned function, we draw it with a scale of 10x applied uniformly. We see that it takes very few (12) neurons to completely represent the function approximated by the network. In fact, the ID pruned function is visually indistinguishable from the full model in this case.

Proof.

$$\eta = \max_{x, W, u} \|u^\top g(W^\top x) - \hat{u}^\top g(\hat{W}^\top x)\|^2$$

For any $x \in \Omega_x$ we have the bound

$$\begin{aligned} \|u^\top g(W^\top x) - \hat{u}^\top g(\hat{W}^\top x)\|^2 &\leq (\|u^\top g(W^\top x)\| + \|\hat{u}^\top g(\hat{W}^\top x)\|)^2 \\ &\leq (\|u^\top g(W^\top x)\| + \|u^\top T^\top g(P^\top W^\top x)\|)^2 \\ &\leq (\|u^\top g(W^\top x)\|(1 + \|T\|))^2. \end{aligned}$$

Therefore,

$$\eta \leq \sup_{x \in \Omega_x} \|u\|_2^2 \|g(W^\top x)\|_2^2 (1 + \|T\|)^2$$

□

Remarks. We can explicitly measure the norm of the interpolation matrix T that appears in the upper bound of Lemma 3.2. Moreover, we expect this to be small because there exists an interpolation matrix such that $t_{ij} \leq 2\forall\{i, j\}$ [35]. The better the interpolation matrix, the better the bound.

D Additional experimental details and results

D.1 Illustrative example

We next give an illustrative example on a synthetic data set where we fully understand the size of a minimum network which can represent the data set. Draw n points iid. from the unit circle in 2 dimensions. Next select 2 (normalized) random vectors v_1 and v_2 . All labels are initialized to zero, and add or subtract 1 to the label for each time it produces a positive inner product with one of the random vectors. With the ReLU activation function it is possible to correctly label all points with a one hidden layer fully connected network of width 4. Construct pairs of neurons, with each pair aligned with the center of one of the random vectors. We can think of the pair as creating a flat function by using one neuron to "cut the top" off of the round part of the function created by the other. We parameterize this with an angle ϕ away from the pair. If each neuron in the pair has the same weight magnitude w , coefficient $\pm u$ and a bias $b \pm \delta/2$, then given a particular w , b and δ , we can write:

$$u(\text{ReLU}(w \cos \phi - b + \delta/2) - \text{ReLU}(w \cos \phi - (b - \delta/2)))$$

As long as $w > b$, this looks like a step function, where the sides get steeper as w approaches infinity. This allows us to perfectly label all of the points given twice the number of neurons as we have random vectors v_1 and v_2 , which is much smaller than the number of data points n .

We train an over-parameterized single hidden layer network to perform fairly well on this task, using an initialization scale that is common in some machine learning platforms such as TensorFlow [41]. This is shown in figure 4. However, magnitude pruning will not necessarily recognize the structure of the minimum representative network because both of the neurons in the pair construction may not have a large magnitude. On this example we see that the interpolative decomposition is able to select neurons which resemble a close to minimal representative network.

D.2 Data set and code licenses

Fashion MNIST [58] is licensed under the MIT License. We are unaware of a license for the CIFAR-10 data set [32]. We adapted code and hyper-parameters from Liu et al. [38] (MIT License), Li et al. [33] (license unaware), and He et al. [20] (license unaware).

D.3 Estimating compute time

The experiments on the illustrative example and Fashion MNIST were performed on a 2019 iMac running an Intel I9. The illustrative example computes in minutes. We trained 15 different model configurations, 8 one hidden layer, and 7 two hidden layer network sizes. For 5 random seeds, we used $5 * (50 + 10 + 10) = 350$ epochs per model size, and trained 15 different model configurations. We used 10,000 images for the pruning set, however, the runtime for computing the ID is cheap compared to training, using the scipy QR decomposition function which calls a LAPACK subroutine [1].

The experiments on CIFAR-10 were performed on a NVIDIA GeForce GTX 1080Ti. For 5 random seeds and two models a total of $5 * 2 * 160 = 1600$ epochs was used for training the ResNet-56 and VGG-16 models. The Table 1 our results required $5 * 3 * 40 = 1200$ epochs of fine-tuning for 5 random seeds and 2 pruning configurations on ResNet-56, 1 configuration on VGG-16. Computing the interpolative decomposition were comparatively cheap, only requiring 1000 data points. The Table 2 and 3 ID results required $5 * 2 * 200 = 2000$ total epochs of fine-tuning for 5 random seeds and 2 different models.

D.4 A difficulty with setting $k(\epsilon)$ in deep networks

By Definition 2.1, an ϵ -accurate interpolative decomposition is associated with a number k of selected columns. We observe that for deep networks it is not straightforward to apply a single accuracy ϵ to the entire network. Figure 5 illustrates the representative variety in the layer-wise singular value decay for a trained VGG-16 model. For our method a sharper singular value decay indicates greater prunability. However, we suspect that this may be misleading in layers that have an incredibly fast initial singular value decay such as layer 13 in figure 5, which would result in pruning almost all of the channels if given a modest accuracy in comparison to earlier layers. With the exception of the initial layer, we observed that layers appear more prunable later in the network as measured by the singular value decay, especially following pooling layers. We believe this is an avenue for future work, however, given the difficulty in determining prunability with deeper networks, we chose to prune constant fractions for this work.

D.5 Ablation studies for design of Algorithm 1

We found that using a held-out pruning set was important to prevent the interpolative decomposition from over-fitting to the training data, and improve generalization performance to the test set. Table 4 reports our results.

In Algorithm 1 we apply the ID from the beginning to the end of the multi-layer network. Doing so one could use the interpolative decomposition to approximate the activation outputs of either the original model or the model. Table 5 gives an ablation study which compares the pruning accuracy for both such cases. We observe that using the ID to approximate the original model achieves higher pruning accuracy (before fine-tuning). We believe that in deep networks there is greater concern for the ID to propagate errors forward through the matrix. Thus by approximating the original model's activation outputs, we can mitigate some of this error propagation.

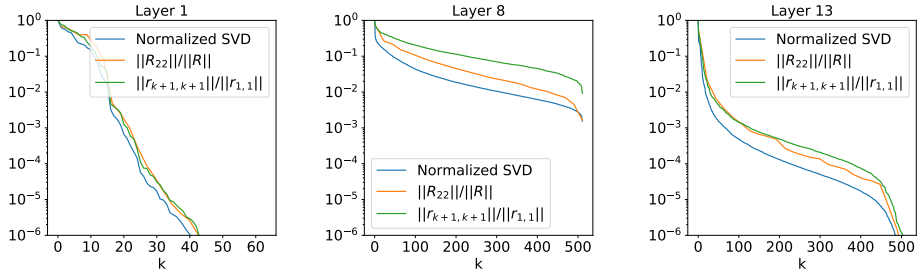


Figure 5: Metrics for different layers in VGG-16. The leftmost layer is the first convolutional layer. The center figure is one of the middle convolutional layers, and the rightmost figure is the last convolutional layer. As we can see, the singular value decay varies throughout the network.

Table 4: Ablation study on the effect of using a held-out (or not) pruning set for the interpolative decomposition. A ResNet-56 model on CIFAR-10 was pruned to 51% FLOPs reduction with a pruning set of 1000. The pruning set was either held-out from the test set, or randomly sampled from the training set. Accuracies are reported as mean and standard deviation over 5 independent trials.

Interpolative Decomposition Pruning Set	Baseline Acc. (%)	Pruning Acc. (%)
Held Out	93.04 (± 0.25)	69.64 (± 2.14)
Not Held Out		66.34 (± 1.30)

D.6 Hyper-parameter details

Fashion MNIST We use a stochastic gradient descent optimizer with a learning rate of 0.3 which decays by a factor of 0.9 for each epoch to train the initial networks. Each was trained for 50 epochs. Our pruning set was 10000 images, which did not need to be held out from training for the simple data set. The fine tuning ran for 10 epochs with an initial learning rate of 0.1 with a decay rate of 0.6 for two layer networks, and 0.2 with a learning rate decay of 0.7 for one layer. Larger ID-pruned models (greater than 512 neurons) can be fine-tuned with a much smaller learning rate of 0.002. These learning rates and number of epochs may not be optimal but were determined through brief empirical tests. We used 5 random seeds for each size of model. The error bars are reported as the uncertainty in the mean, defined in terms of the standard deviation σ , and number of independent trials N , $\sigma_{mean} = \sigma/\sqrt{N}$.

CIFAR-10 The VGG-16 and ResNet-56 models are trained with 5 random seeds and with hyper-parameter specifications and code provided by Liu et al. [38]. The test set is randomly partitioned into a prune set and new test set. In Table 1: For magnitude pruning we use the hyper-parameters specified by Liu et al. [38] to fine-tune for 40 epochs and learning rate 0.001. The interpolative decomposition uses a held out pruning set of 1000 data points and the same fine-tuning hyper-parameters, except the

Table 5: Ablation study on the effect of approximating the activation outputs of the original or pruned model using the interpolative decomposition. A ResNet-56 model on CIFAR-10 was pruned to 51% FLOPs reduction with a held-out pruning set of size 1000. Accuracies are reported as mean and standard deviation over 5 independent trials.

Interpolative Decomposition Approximation Target	Baseline Acc. (%)	Pruning Acc. (%)
Original Model	93.04 (± 0.25)	69.64 (± 2.14)
Pruned Model		63.19 (± 4.66)

ResNet-56 is retrained with initial learning rate 0.01 and decreased to 0.001 after 10 epochs. The VGG-16 uses the same hyper-parameters as [38].

For Tables 2 and 3, we implement the method by He et al. [20] with their provided code and hyper-parameter settings on our trained models to fine-tune for 200 epochs. The interpolative decomposition uses a held out pruning set of 1000 data points with a hyper-parameter configuration from He et al. [20]: use a starting learning rate 0.1 decaying to 0.02, 0.004, 0.0008 at epochs 60, 120, 160 to train for 200 epochs total with batch size 128 and weight decay $5e-4$.